Journal of the Serbian Chemical Society
JSCS@tmf.bg.ac.rs • www.shd.org.rs/JSCS

J. Serb. Chem. Soc. 75 (1) 61–74 (2010)
JSCS–3941

UDC 742+547.52+547.7–36+547.884.2:548.58
Original scientific paper

Synthesis, characterization and DNA cleavage activity of nickel(II) adducts with aromatic heterocyclic bases

M. S. SURENDRA BABU[1], PITCHIKA G. KRISHNA[2], K. HUSSAIN REDDY[1]* and G. H. PHILIP[2]

[1]*Department of Chemistry, Sri Krishnadevaraya University, Anantapur-515003 and* [2]*Department of Zoology, Sri Krishnadevaraya University, Anantapur-515003, India*

(Received 21 January, revised 7 October 2009)

Abstract: Mixed ligand complexes of nickel(II) with 2,4-dihydroxyacetophenone oxime (DAPO) and 2,4-dihydroxybenzophenone oxime (DBPO) as primary ligands, and pyridine (Py) and imidazole (Im) as secondary ligands were synthesized and characterized by molar conductivity, magnetic moments measurements, as well as by electronic, IR, and ^{1}H-NMR spectroscopy. Electrochemical studies were performed by cyclic voltammetry. The active signals are assignable to the $Ni^{III/II}$ and $Ni^{II/I}$ redox couples. The binding interactions between the metal complexes and calf thymus DNA were investigated by absorption and thermal denaturation. The cleavage activity of the complexes was determined using double-stranded pBR322 circular plasmid DNA by gel electrophoresis. All complexes showed increased nuclease activity in the presence of the oxidant H_2O_2. The nuclease activities of mixed ligand complexes were compared with those of the parent copper(II) complexes.

Keywords: Ni(II) complexes; oximes; mixed ligands; DNA interaction; cleavage activity.

INTRODUCTION

Studies on the chemical modification of nucleic acids by transition metal complexes are of paramount importance for designing chemotherapeutic drugs, regulating gene expression and designing tools for molecular biology.[1–6] Many coordination compounds of transition metal ions accomplish nucleolytic cleavage. Nickel is a remarkably versatile metal in biological chemistry. It is a necessary component of certain metallo-proteins but simultaneously an environmental carcinogen causing DNA damage and protein–DNA crosslinks. Nickel compounds have two characteristics in common with leading antitumour drugs: direct metal binding to N7 of guanine is possible and nickel complexes are able

* Corresponding author. E-mail: manabolu@gmail.com
doi: 10.2298/JSC1001061B

to catalyze oxidative damage to nucleic acids.[7–9] It was found that high-valent nickel species may also mediate through sequence-specific oxidative cleavage of DNA by designed metallo-proteins.[10] A number of authors have concluded that Ni^{2+} binds covalently to the N7 atom of guanine and adenine.[11–13] Nickel-induced carcinogenesis involves the oxidation of Ni^{2+} to Ni^{3+} by intracellular oxidants, such as H_2O_2.[14] This oxidation of nickel, presumably through Fenton-type reactions, results in the formation of reactive oxygen species, which can then cause oxidative damage to DNA. Recent reports on the nucleolytic activity of oxime complexes[15,16] prompted us to investigate the structural peculiarities and nuclease activity of Ni(II) oxime complexes and aromatic base(pyridine/imidazole) adducts.

EXPERIMENTAL

Apparatus and reagents

2,4-Dihydroxyacetophenone and 2,4-dihydroxybenzophenone were purchased from Merck and the metals used in the preparation of the complexes were of reagent grade. The solvents used in the synthesis of the ligands and metal complexes were distilled before use. All other chemicals were of AR grade and were used without further purification. Agarose, used in gel electrophoresis, was purchased from Sigma-Aldrich. Calf thymus DNA (CT DNA) and plasmid pBR322 were purchased from Genie Biolabs, Bangalore, India. The elemental analyses were performed using a Perkin-Elmer 2400 CHNS elemental analyzer. The magnetic moments were determined in the polycrystalline state using a PAR model-155 vibrating sample magnetometer operating at a field strength of 2–8 kG. Nickel of high purity (saturation moment 55 e.m.u./g) was used as the standard. The molar conductance of the complexes in DMF (10^{-3} M) solution was measured at 28±2 °C with a Systronic model 303 direct-reading conductivity bridge. The electronic spectra were recorded in DMF employing a Shimadzu UV-160A spectrophotometer. The FTIR spectra were recorded in the range 4000–50 cm^{-1} with a Bruker IFS 66V in KBr discs and polyethylene medium. The ^{1}H-NMR spectra of parent complexes in DMSO-d_6 solvent were recorded on JEOL GSX 400NB multinuclear FT--NMR spectroscope at SAIF, IIT, Madras. The voltammetric measurements were performed using a Bio-Analytical System (BAS) CV-27 assembly in conjunction with an *x–y* recorder. The measurements were made on degassed (N_2 bubbling for 5 min) solutions in DMF (10^{-3} M) containing 0.10 M tetraethylammonium perchlorate as the supporting electrolyte. The three-electrode system consisted of a glassy carbon (working), platinum (auxiliary) and Ag/ /AgCl (reference) electrodes.

Synthesis of complexes

$Ni(DAPO)_2$ (**1**) was prepared by mixing $NiCl_2$ (4.3 g, 0.025 mol) and 2,4-dihydroxyacetophenone (8.3 g, 0.050 mol) in a 1:2 ratio in 50 % aqueous ethanolic medium. The reaction mixture was maintained at pH 8 using 1.0 M sodium acetate solution and stirred for 30 min. The obtained green precipitate was filtered, washed with hot water and cold methanol. The complex was dried at 110 °C.

$Ni(DBPO)_2$ (**2**) was prepared as described above, but using 2,4-dihydroxybenzophenone to afford a thick green precipitate.

$[Ni(DAPO)_2Py_2]$ (**3**) was synthesised by dissolving the nickel(II) complex of DAPO (3.0 g, 0.018 mol) in pyridine (3.0 ml) in a Schlenk tube. The solution was stirred magnetically for

30 min and *n*-hexane (25 ml) was added. After standing at room temperature for 3–4 days, a dark green product formed which was filtered, washed with water and *n*-hexane and dried under reduced pressure over $CaCl_2$.

$[Ni(DBPO)_2Py_2]$ (**4**) was prepared by dissolving the nickel(II) complex of DBPO (0.60 g, 0.026 mol) in pyridine (10 ml) in a schlenk tube. The solution was stirred magnetically for 30 min and *n*-hexane (25 ml) was added. After standing at room temperature for 7 days, a dark green product formed which was filtered, washed with water and *n*-hexane and dried under reduced pressure over $CaCl_2$.

$[Ni(DAPO)_2Im_2]$ (**5**) was prepared by placing the nickel(II) complex of DAPO (1.67 g, 0.0100 mol) in a 250 ml round bottom flask. Imidazole (3.4 g, 0.050 mol) dissolved in 30 ml of CH_2Cl_2 was added to the contents of the flask. The reaction mixture was refluxed on a water bath for 2 h. On cooling, a dark green precipitate formed which was filtered, washed with cold *n*-hexane and dried under vacuo over $CaCl_2$.

$[Ni(DBPO)_2Im_2]$ (**6**) was synthesised by placing the nickel(II) complex of DBPO (0.010 mol) in a 250 ml round bottom flask. Imidazole (0.050 mol) dissolved in 30 ml of CH_2Cl_2 was added to the contents of the flask. The reaction mixture was refluxed on a water bath for 2 h. On cooling, a dark green precipitate formed which was filtered, washed with cold *n*-hexane and dried under vacuum over anhydrous $CaCl_2$.

DNA binding and cleavage experiments

All measurements with CT DNA were performed in buffer Tris–HCl 5 mM (pH 7.2), 50 mM NaCl. The UV absorbance ratio $\lambda_{260}/\lambda_{280}$ was 1.8–1.9, indicating the DNA was sufficiently free of protein.[13] The concentration of CT DNA per nucleotide was determined from the absorption intensity at 260 nm with the known ε value of 6600 M^{-1} cm^{-1}.[17] The absorption titrations were performed by adding increasing amounts of CT DNA to a solution of the complex at a fixed concentration contained in a quartz cell and recording the UV–Vis spectrum after each addition. The absorption of CT DNA was subtracted by adding the same amounts of DNA to a blank. The data were then fitted to Eq. (1) to obtain the intrinsic binding constant, K_b.[18]

$$[DNA] / (\varepsilon_a - \varepsilon_f) = [DNA] / (\varepsilon_b - \varepsilon_f) + 1/K_b(\varepsilon_b - \varepsilon_f) \quad (1)$$

where ε_a, ε_f and ε_b are the apparent, free and bound metal complex extinction coefficients, respectively. A plot of $[DNA] / (\varepsilon_a - \varepsilon_f)$ *vs*. [DNA] gave a slope of $1/(\varepsilon_b - \varepsilon_f)$ and a *y*-intercept equal to $1/K_b(\varepsilon_b - \varepsilon_f)$. Thus, K_b is the ratio of the slope to the *y*-intercept.

DNA melting experiments were performed using a spectrophotometer connected to a thermostat. The absorbance of DNA (75 μM) at 25–80 °C in both the absence and presence of 7.5 μM of the complex was recorded at 260 nm. The melting temperature (T_m) was calculated by plotting the temperature *vs*. the relative absorption intensity (A/A_0).

A DMF solution containing the metal complexes (10 μM) in a clean Eppendorf tube was treated with pBR322 plasmid DNA (3.3 μl of 150 μg/ml) in Tris-HCl buffer (0.10 M, pH 8.0) containing NaCl (50 mM) in presence and absence of additives. The contents were incubated for 1 h at 37 °C and loaded onto a 1 % agarose gel after mixing 5 μl of loading buffer (0.25 % bromophenol blue + 25 % xylene cyanol + 30 % glycerol, sterilized distilled). The electrophoresis was performed at a constant voltage (80 V) until the bromophenol blue had travelled through 75 % of the gel. Subsequently, the gel was stained for 10 min by immersion in ethidium bromide solution. The gel was then destained for 10 min by keeping it in sterile distilled water. The plasmid bands were visualized by viewing the gel under a transilluminator and photographed.

RESULTS AND DISCUSSION

Nickel complexes were prepared using oxime ligands with nickel chloride, and further with pyridine and imidazole to form mixed ligand complexes. All the complexes were freely soluble in DMF and DMSO, slightly soluble in methanol and ethanol, and insoluble in water.

The evaluated analytic and spectroscopic characteristics of the prepared complexes are given below

Ni(DAPO)$_2$ ***(1)***. Yield: 81 %; m.p.: 198–202 °C. Anal. Calcd. for $C_{16}H_{16}N_2O_6Ni$: C, 49.16; H, 4.12; N, 7.12 %; found: C, 49.36; H, 4.10; N, 7.11 %. FTIR (KBr, cm^{-1}): 1605 (C=N), 458 (N–Ni), 523 (O–Ni). ^{1}H-NMR ($CDCl_3$, δ / ppm): 2.0 (3H, *s*, CH_3), 6.2–6.4 (2H, *dd*, Ar, J = 3.4 Hz), 7.2 (1H, *d*, Ar J = = 6.2 Hz), 9.6 (1H, *s*, OH), 11.8 (1H, *s*, oxime OH).

Ni(DBPO)$_2$ ***(2)***. Yield: 63 %; m.p.: 256–260 °C. Anal. Calcd. for $C_{26}H_{18}N_2O_6Ni$: C, 60.42; H, 3.91; N, 5.41 %; found: C, 60.25; H, 3.92; N, 5.32 %. FTIR (KBr, cm^{-1}): 1614 (C=N), 455 (N–Ni), 576 (O–Ni). ^{1}H-NMR (δ / ppm): 6.2–6.4 (3H, *m*, Ar), 7.2 (5H, *m*, Ar), 10.6 (1H, *br s*, phenolic OH),12.4 (1H, *s*, oxime OH).

[Ni(DAPO)$_2$Py$_2$] ***(3)***. Yield: 42 %; m.p: 170–172 °C. Anal. Calcd. for $C_{26}H_{26}N_4O_6Ni$: C, 56.82; H, 4.77; N, 10.2 %; found: C, 56.91; H, 4.78; N, 10.6 %. FTIR (KBr, cm^{-1}): 1600 (C=N), 472 (N–Ni), 690 (N–Ni of Py), 548 (O–Ni).

[Ni(DBPO)$_2$Py$_2$] ***(4)***. Yield: 38 %; m.p.: 212–214 °C. Anal. Calcd. for $C_{36}H_{30}N_4O_6Ni$: C, 64.21; H, 4.49; N, 8.73 %; found: C, 64.25; H, 4.46; N, 8.71 %. FTIR (KBr, cm^{-1}): 1613 (C=N), 460 (N–Ni), 699 (N–Ni of Py), 565 (O–Ni).

[Ni(DAPO)$_2$Im$_2$] ***(5)***. Yield: 65 %; m.p.: 118–190 °C. Anal. Calcd. for $C_{22}H_{24}N_6O_6Ni$: C, 50.18; H, 4.59; N, 15.9 %; found: C, 50.18; H, 4.52; N, 15.72 %. FTIR (KBr, cm^{-1}): 1590 (C=N), 472 (N–Ni), 710 (N–Ni of Im), 562 (O–Ni).

[Ni(DBPO)$_2$Im$_2$] ***(6)***. Yield: 49 %; m.p.: 198–202 °C. Anal. Calcd. for $C_{32}H_{28}N_6O_6Ni$: C, 59.01; H, 4.33; N, 12.9 %; found: C, 58.72; H, 4.32; N,12.8 %. FTIR (KBr, cm^{-1}): 1595 (C=N), 475 (N–Ni), 715 (N–Ni of Im), 560 (O–Ni).

The elemental analysis supported the 1:2 compositions of the metal and ligands. The molar conductance data of these nickel complexes suggested their non-electrolytic nature (Table I). The magnetic moment values of the parent complexes suggested that they are diamagnetic, while the corresponding pyridine and imidazole complexes, having a magnetic momentum in range 3.0–3.6 μ_B, were paramagnetic and favoured octahedral geometry with a $^3A_{2g}$ ground state.

The electronic spectra of the studied Ni(II) complexes are given in Fig. 1. The electronic spectra of all complexes consisted of three bands: one at ≈10000 cm^{-1} due to $^3A_{2g} \rightarrow {}^3T_{2g}$ (ν_1), ≈17000 cm^{-1} due to $^3A_{2g} \rightarrow {}^3T_{1g}$ (ν_2) and ≈29000 cm^{-1} due to $^3A_{2g} \rightarrow {}^3T_{2g}$ (ν_3), which clearly indicates octahedral stereochemistry. The spectral data were utilized to compute important ligand field parameters (10 *Dq* and *B*) using the ligand field of spin allowed transitions in the d^8

configuration. The values of 10 *Dq* and the Racah interelectronic repulsion parameter (*B*) were employed to calculate ν_2 and ν_3 and the results are given in Table II.

TABLE I. Magnetic moment and molar conductivity data of Ni(II) complexes and adducts **1**–**4**

Compound	Complex	Molar conductance, S cm^2 mol^{-1}	Magnetic moment μ_{eff} / μ_B
1	$[Ni(DAPO)_2]$[a]	15.4	Diamagnetic
2	$[Ni(DAPO)_2Py_2]$[b]	13.4	3.16
3	$[Ni(DAPO)_2Im_2]$[c,d]	12.2	3.18
4	$[Ni(DBPO)_2]$[e]	8.8	Diamagnetic
5	$[Ni(DBPO)_2Py_2]$	7.4	2.89
6	$[Ni(DBPO)_2Im_2]$[d]	7.2	2.93

[a]DAPO = 2,4-dihydroxyacetophenone oxime; [b]Py = pyridine; [c]Im = imidazole; [d]decomposes on staying for more than 32 h in DMF solution; [e]DBPO = 2,4-dihydroxybenzophenone oxime

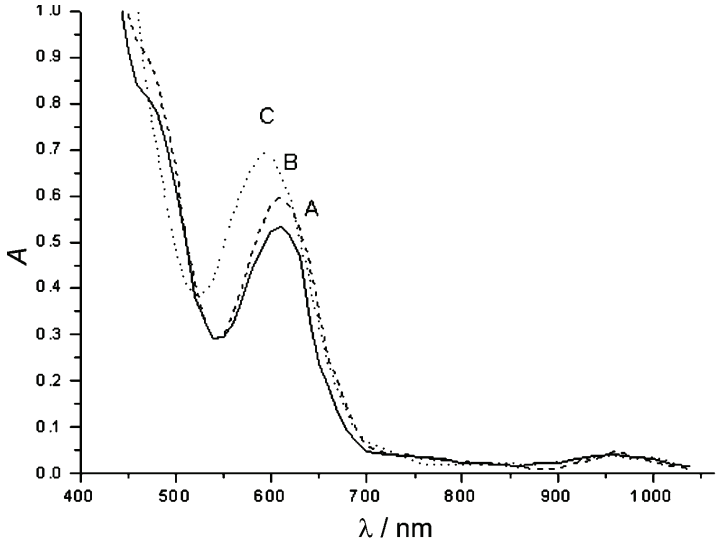

Fig. 1. Electronic spectra of the complexes, a) $[Ni(DAPO)_2]$, b) $[Ni(DAPO)_2Py_2]$ and c) $[Ni(DAPO)_2Im_2]$.

Comparison of the 10*Dq* and *B* values indicates that the ligands formed reasonably strong covalent bonds within the complexes. The high values of 10*Dq* and *B* are also consistent with coordination of the oxime nitrogen. The ratios of ν_1 and ν_2 lie between 1.56–1.68, as expected for octahedral nickel(II) complexes.[19] The Racah interelectronic repulsion parameters (*B*) and the covalent factor (B_{35}) are used for establishing the position of the present ligands in a nephelauxetic series. The data for these complexes gave h_x values from 0.90 to 1.19, suggesting that the present ligands may be placed between water and ammonia. As the *LSFE* values of the complexes were nearly the same, they reflected almost identical coordination around the central metal ion.

TABLE II. Electronic spectral data (cm^{-1}) and ligand field parameters of the studied Ni(II) complexes

Complex	Method of evaluations	ν_1	ν_2	ν_3	β	Δ	B_{35}	10 Dq	$\nu_2-\nu_1$	ν_2/ν_1	$LFSE$	h_x
$[Ni(DAPO^a)_2]$	Observed	10760	16660	28980	890.6	649	0.89	10760	5900	1.54	30.74	1.07
	Calculated	10Dq	17301	28331					6541	1.60		
$[Ni(DAPO)_2Py_2]$	Observed	10790	16950	28980	904	432	0.87	10790	6160	1.57	30.80	1.09
	Calculated	10Dq	17381	28548					6591	1.61		
$[Ni(DAPO)_2Im_2]$	Observed	10820	17120	28750	934.2	562	0.82	10820	6308	1.64	29.25	1.05
	Calculated	10Dq	17840	29650					6060	1.61		
$[Ni(DBPO^b)_2]$	Observed	10790	16780	29185	902.1	601	0.88	10790	5990	1.54	30.82	1.10
	Calculated	10Dq	17376	28524					6586	1.61		
$[Ni(DBPO)_2Py_2^c]$	Observed	10810	16890	29225	912.3	542	0.89	10810	6080	1.56	30.89	1.11
	Calculated	10Dq	17433	28683					6623	1.61		
$[Ni(DBPO)_2Im_2^d]$	Observed	10820	17240	29250	933.6	561	0.82	10820	6420	1.60	30.54	1.10
	Calculated	10Dq	17840	29650					7020	1.64		

[a]2,4-dihydroxyacetophenone oxime; [b]2,4-dihydroxybenzophenone oxime; [c]pyridine, [d]imidazole

Important IR spectral band data of the nickel(II) complexes are present in Table III. The ν_{OH} stretching vibrations of phenolic groups observed at 3200––3000 cm^{-1} in the spectra of the ligands are absent in the spectra of the complexes, suggesting that the phenolic oxygen is coordinated to the metal. The $\nu_{C=N}$ band observed at 1620–1630 cm^{-1} in the spectra of the ligands is shifted to lower frequency in those of the complexes and adducts. This indicates that the metal coordinates to the nitrogen of the oxime group. The band at 1550–1530 cm^{-1} is assigned to $\nu_{C=N}$ stretching in pyridine and imidazole. An absorption band appearing around 3400 cm^{-1} in the complexes of DAPO and DBPO is assigned to the free phenolic –OH group present in the *para* position of the aromatic ring. A broad and nearly flat band present in the region 3000–2900 cm^{-1} indicates that the oxime OH proton is not released during the formation of the metal chelates. The shape of this band in the metal chelates can be attributed to intramolecular hydrogen bonding, which lies in a plane, suggesting the formation of very stable five--membered rings. The non-ligand absorptions in the regions 470–450 cm^{-1} and 570–520 cm^{-1} are tentatively assigned to ν_{M-N} and ν_{M-O}, respectively. The strong absorption band at 260–220 cm^{-1} is absent in the spectra of the metal complexes but appeared in the adducts; a weak band also appeared in region 650–730 cm^{-1}. These bands are assigned to the ν_{M-N} (pyridine/imidazole) vibrational mode, indicating the presence of pyridine/imidazole in coordination with nickel in the adducts.

TABLE III. Selected IR bands (cm^{-1}) of the studied Ni(II) complexes with tentative assignment (*vs* = very strong, *s* = strong, *m* = medium, *w* = weak)

Complex	ν_{OH} (oxime)	$\nu_{C=N}$	$\nu_{C=N}$ (Py/Im)	ν_{M-N}	ν_{M-N} (Py/Im)	ν_{M-O}
$[Ni(DAPO)_2]$	3290 *s*	1605 *vs*	–	468 *w*	–	592 *w*
$[Ni(DAPO)_2(Py)_2]$	3350 *s*	1600 *s*	1555 *w*	472 *w*	690 *m*	562 *w*
$[Ni(DAPO)_2(Im)_2]$	3330 *s*	1590 *s*	1560 *w*	476 *w*	710 *m*	548 *w*
$[Ni(DBPO)_2]$	3300 *s*	1614 *vs*	–	455 *w*	–	576 *w*
$[Ni(DBPO)_2(Py)_2]$	3320 *s*	1613 *s*	1545 *w*	460 *w*	699 *m*	–
$[Ni(DBPO)_2(Im)_2]$	3310 *s*	1612 *s*	1560 *w*	455 *w*	705 *m*	568 *w*

The ^{1}H-NMR spectra of parent complexes were taken in DMSO-d_6. The phenolic proton peaks present in the spectra of the ligands are absent in the ^{1}H-NMR spectra of all complexes, suggesting coordination of the phenolic oxygen to the metal.

Based on the elemental analysis, magnetic moments, electronic, IR and ^{1}H--NMR data, tentative structures of the complexes and adducts are given in Fig. 2a and 2b, respectively.

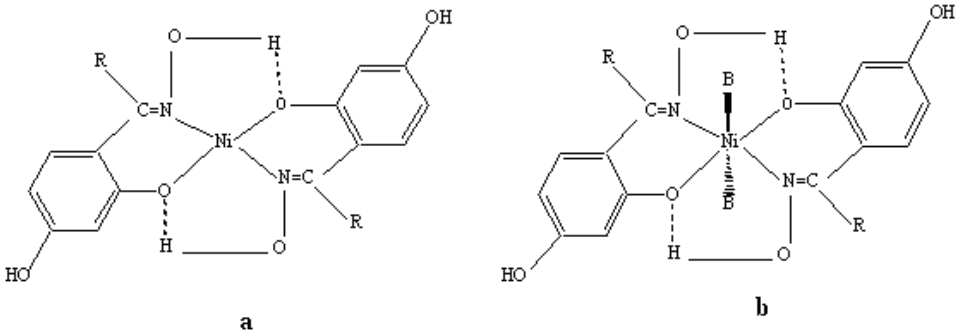

Fig. 2. a) Structure of the nickel(II) complexes, where R = CH_3 – 2,4-dihydroxyacetophenone oxime (DAPO) or R = C_6H_5 – 2,4-dihydroxybenzophenone oxime (DBPO) and b) structure of the nickel(II) adducts, where R = CH_3 – 2,4-dihydroxyacetophenone oxime (DAPO) or C_6H_5 – 2,4-dihydroxybenzophenone oxime (DBPO) and B = pyridine or imidazole.

Cyclic voltammetry

The oxidation–reduction potentials of the nickel ion in the complexes were studied by cyclic voltammetry. The cyclic voltammograms of the nickel(II) complexes were recorded in DMF containing tetraethylammonium perchlorate (0.10 M) as the supporting electrolyte. The cyclic voltammetric profiles of representtative complexes are given in Fig. 3. The electrochemical data of all complexes obtained at the glassy carbon electrode in DMF are given in Table IV. The redox behaviour of the nickel(II) complexes showed two active responses by cyclic voltammetry. The $E_{1/2}$ values of the nickel complexes were observed in the potential range –1.75 to –1.45 *vs.* Ag/AgCl, assigned to the $Ni^{III/II}$ couple and in the potential range –1.50 to –0.95 V *vs.* Ag/AgCl, assigned to $Ni^{II/I}$. Repeated scans as well as various scan rates showed that dissociation did not occur in these complexes. The large non-equivalence of the current intensity of the cathodic and anodic peaks indicates the quasi-reversible behaviour of these complexes. The ΔE_p values were greater than the Nernstian values ($\Delta E_p \approx 59$ mV) for a one--electron redox system. This indicates a considerable reorganization of the coordination sphere during electron transfer, as was observed for a number of other nickel (II) complexes. As can be seen from Table IV, the pyridine and imidazole adducts had higher $E_{1/2}$ values than the parent complexes, showing that the addition of the second ligand slightly destabilized the Ni(II) oxidation state. The $\Delta G^{\ominus}$ values of the mixed ligand complexes were lower than those of the parent complexes, showing that the adducts were less stable than the parent complexes.

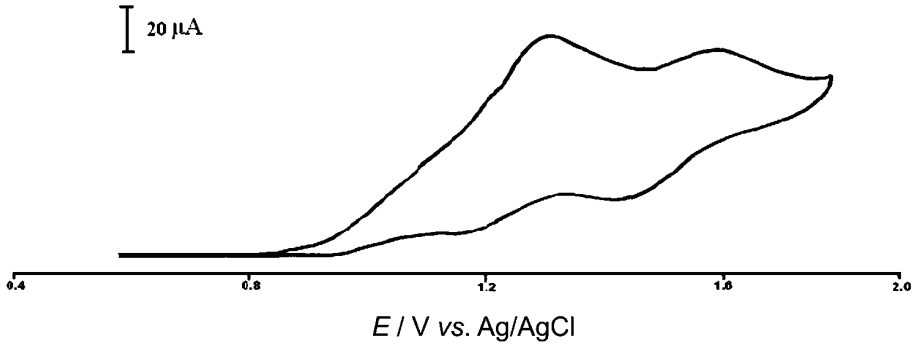

Fig. 3. Cyclic voltammogram of $[Ni(DAPO)_2Im_2]$ at a scan rate of 50 mV s^{-1}.

A comparison of the $E_{1/2}$ values of this redox couple of the present complexes with other analogous nitrogen donor macrocycles revealed that the oxime complexes undergo a more facile redox change, which seems to be a requirement for DNA cleavage.[20]

TABLE IV. Cyclic voltammetric data of the Ni(II) DAPO and DBPO complexes with or without pyridine/imidazole ligands (recorded in DMF at room temperature with Et_4NClO_4 as the supporting electrolyte; glassy carbon as the working electrode, Pt wire as the auxiliary electrode and Ag/AgCl as the reference electrode; scan rate: 50 mV s^{-1})

Complex	Redox couple	$E_{p,c}$ / V	$E_{p,a}$ / V	ΔE_p / mV	$E_{1/2}$ / V	log K_c[a]	$-\Delta G^{\ominus}$[b] / kJ mol^{-1}
$[Ni(DAPO)_2]$	III/II	–1.52	–1.45	70	–1.48	–	–
	II/I	–1.25	–0.97	280	–1.11	9.31	54
$[Ni(DAPO)_2(Py)_2]$	III/II	–1.48	–1.45	30	–1.47	–	–
	II/I	–1.19	–0.89	300	–1.04	9.97	58
$[Ni(DAPO)_2(Im)_2]$	III/II	–1.54	–1.41	130	–1.47	4.32	25
	II/I	–1.20	–0.94	260	–1.07	8.64	50
$[Ni(DBPO)_2]$	III/II	–1.64	–1.53	110	–1.58	3.66	22
	II/I	–1.37	–1.12	250	–1.25	8.31	48
$[Ni(DBPO)_2(Py)_2]$	III/II	–1.72	–1.58	140	–1.65	4.65	27
	II/I	–1.33	–1.09	240	–1.21	7.98	46
$[Ni(DBPO)_2(Im)_2]$	III/II	–1.74	–1.58	160	–1.66	4.68	28
	II/I	–1.34	–1.10	240	–1.22	7.98	46

[a]$\log K_c = 0.434nF/RT\Delta E_p$; [b]$\Delta G^{\ominus} = -2.303RT\log K_c$

Binding of the nickel(II) complexes with CT DNA

The interaction of the nickel(II) complexes with CT DNA was monitored by UV–Vis spectroscopy in the 265–280 nm and 300–315 nm regions. In the presence of increasing amounts of CT DNA, the spectra of all the complexes showed a decrease in the intensity of the bands in the case of parent complexes and increase in the intensity for the mixed ligand complexes (Fig. 4). However, the bands are shifted towards lower wavelengths (blue shift). The change in absorbance va-

lues with increasing amount of CT DNA were used to evaluate the intrinsic binding constant K_b for the complexes.

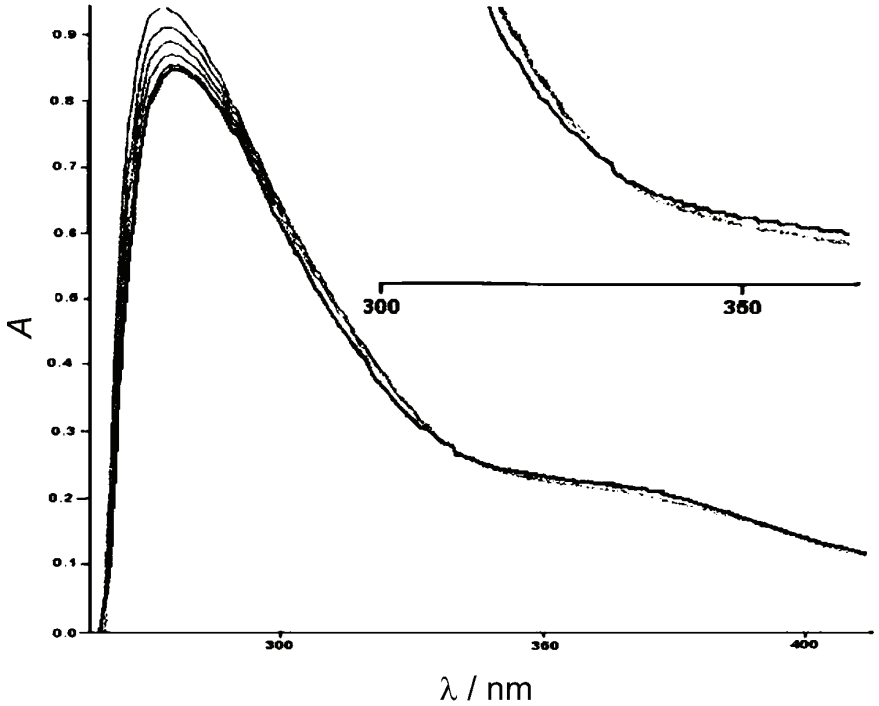

Fig. 4. UV–Vis spectra of $[Ni(DAPO)_2Im_2]$ (37±0.5 μM) in the absence (dotted line) and presence of increasing amounts of CT DNA. Portion of the graph showing an isosbestic point at 337 nm is given in the inset.

In the presence of increasing amounts of CT DNA, the UV–Vis absorption of $Ni(DAPO)_2$ and $Ni(DBPO)_2$ showed hypsochromic shifts ($\Delta\lambda_{max}$: 0.5 to 5.0 nm) and hypochromism [hypochromicity: –7.4 % for $Ni(DAPO)_2$ and –12.4 % for $Ni(DBPO)_2$]. $Ni(DBPO)_2$ exhibited the highest percentage hypochromic shift and binding constant of all the parent complexes. In contrast, the mixed ligand complexes showed hyperchromic shifts with increasing amounts of calf thymus DNA. The pyridine adducts of $Ni(DAPO)_2$ and $Ni(DBPO)_2$ showed hyperchromicity of 6.5 and 11.8, respectively, while for the imidazole adducts, these values were 5.8 and 5.6. The change in hypochromic shifts to hyperchromic shifts when going from the parent complexes to the mixed ligand complexes suggest a change in the mode of DNA binding. This may be attributed to the change in the structure from square planar (parent complexes) to octahedral (mixed ligand complexes). The order of the binding of the complexes with DNA is as follows:

$Ni(DBPO)_2Im_2$ (2.6×10^6) > $Ni(DAPO)_2Im_2$ (2.4×10^6) > $Ni(DBPO)_2Py_2$ (1.8×10^6) > $Ni(DAPO)_2Py_2$ (1.6×10^6) > $Ni(DBPO)_2$ (3.4×10^5) > $Ni(DAPO)_2$ (2.9×10^5).

The strong DNA binding nature of the octahedral mixed ligand nickel complexes may be due to the additional π–π interactions through the aromatic ring of the nitrogen bases. The binding constants of the square planar parent complexes are also sufficiently high, possibly due to an intercalation mode of binding.[21]

Thermal denaturation

The binding of small molecules into the DNA double helix is known to increase the melting temperature of the helix, which is the temperature at which the double helix is denatured into single stranded DNA.[22] The value of extinction coefficient of the DNA bases at 260 nm in the double helical form is lower than in the single stranded form. Hence, melting of the helix leads to an increase in the absorption at this wavelength. Thus, the transition temperature from helix to coil can be determined by monitoring the absorbance of the DNA bases at 260 nm.

The thermal melting studies were performed at [DNA]/[complex] = 25. The T_m values were determined by monitoring the absorbance of DNA at 260 nm as a function of temperature. The melting point of free CT-DNA was 60±1 °C under the employed experimental conditions. Under the same set of conditions, addition of $Ni(DAPO)_2$, $Ni(DAPO)_2Py_2$ and $Ni(DAPO)_2Im_2$ increased T_m (±1 °C) by 3, 5 and 6 °C, respectively, while $Ni(DBPO)_2$, $Ni(DBPO)_2Py_2$ and $Ni(DBPO)_2Im_2$ increased T_m (±1 °C) by 4, 5 and 7 °C, respectively. These increases of the T_m values of CT-DNA in the presence of the complexes indicated that these compounds stabilized the double helix of DNA.[23]

Cleavage activity of pBR322 plasmid DNA

Gel electrophoresis experiments using pBR322 circular plasmid DNA were performed with the ligands and complexes in the presence and absence of H_2O_2 as an oxidant. At micromolar concentrations for a 2 h incubation period, the ligands exhibited no significant cleavage activity in the absence and in presence of the oxidant (H_2O_2). The nuclease activity was greatly enhanced by the incorporation of the nickel ion into the respective ligands.

The cleavage activities of the nickel complexes on pBR322 are shown in Fig. 5. In Fig. 5, lanes 1 and 2 are controls while the other lanes contain nickel complexes in presence (odd lanes) and absence (even lanes) of oxidant (H_2O_2). The nickel complexes of DAPO and DBPO were run in lanes 3 and 4, and 9 and 10, respectively. It is clear that the parent complexes did not show a significant cleavage activity even in presence of the oxidant. Lanes 5 and 6, and 11 and 12 contained the pyridine adducts of $Ni(DAPO)_2$ and $Ni(DBPO)_2$, respectively, in the presence and absence of oxidant. Both adducts converted form I (super coiled) into form II (nicked). The cleavage activity of the nickel adducts was signifi-

cantly increased in the presence of the oxidant (H_2O_2). Similarly, the imidazole adducts also showed higher cleavage activity in the presence of oxidant. In lanes 13 and 14, containing $Ni(DBPO)_2Im_2$, significant cleavage activity was observed, while both form I and II were converted into smears in the presence of oxidant.

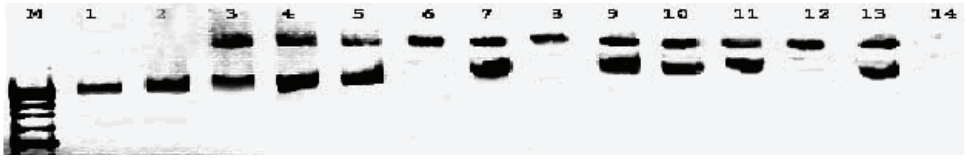

Fig. 5. Agarose gel (1 %) showing the results of electrophoresis of 3.3 µl of (150 µg ml^{-1}) pBR322 plasmid DNA, 2 µl of 0.1 M Tris-HCl (pH 8.0) buffer: 1 µl (1 mM) complex in DMF; 10 µl of sterilized water and 2 µl of 9.0 mM H_2O_2 were added, respectively, incubation at 37 °C (60 min); lane M : Marker, lane 1: DNA (control); lane 2: DNA + H_2O_2 (control); lane 3: $[Ni(DAPO)_2]$; lane 4: $[Ni(DAPO)_2] + H_2O_2$; lane 5: $[Ni(DAPO)_2Py_2]$; lane 6: $[Ni(DAPO)_2Py_2] + H_2O_2$; lane 7: $[Ni(DAPO)_2Im_2]$; lane 8: $[Ni(DAPO)_2Im_2] + H_2O_2$; lane 9: $[Ni(DBPO)_2]$; lane 10: $[Ni(DBPO)_2] + H_2O_2$; lane 11: $[Ni(DBPO)_2Py_2]$; lane 12: $[Ni(DBPO)_2Py_2] + H_2O_2$; lane 13: $[Ni(DBPO)_2Im_2]$; lane 14: $[Ni(DBPO)_2Im_2] + H_2O_2$.

From Fig. 5, it is evident that the $Ni(DBPO)_2Im_2$ complex showed significant cleavage activity in the presence of the oxidant. This may be attributed to the formation of hydroxyl free radicals, which oxidized Ni(II) to Ni(III), presumably through Fenton-type reactions, resulting in the formation of reactive oxygen species, which could then cause oxidative damage to DNA.[24]

CONCLUSIONS

Mixed ligand complexes having the formulae $Ni(L)_2L^1_2$ (where L = DAPO or DBPO and L^1 = pyridine (Py) or imidazole (Im)) were synthesized and characterized by magnetic susceptibility and elemental analysis, as well as by UV–Vis, IR and ^{1}H-NMR spectroscopy. The electronic spectral data suggested a square planar structure for the parent complexes and an octahedral structure for the adducts. The electrochemical data of these complexes, realised by cyclic voltammetry, showed the redox couple Ni^{III}/Ni^{II}. Absorption titrations were performed on CT DNA to study the binding nature. The values of the binding constant were sufficiently high (10^6) and comparable to other mixed ligands.[25] Both the binding constant and thermal denaturation studies suggested that these complexes bind to CT DNA by an intercalative mechanism.[26] The DNA cleavage activity of the nickel complexes determined on double-stranded pBR322 circular plasmid DNA showed that these complexes cleave DNA by an oxidation mechanism, mainly through a Fenton reaction.

Acknowledgments. The financial support received from the University Grant Commission, New Delhi, India (F12-118/2001) is gratefully acknowledged.

ИЗВОД

СИНТЕЗА, КАРАКТЕРИЗАЦИЈА И АКТИВНОСТ НИКАЛ(II) АДУКАТА СА АРОМАТИЧНИМ ХЕТЕРОЦИКЛИЧНИМ БАЗАМА ПРЕМА РАСКИДАЊУ DNA

M. S.SURENDRA BABU[1], PITCHIKA. G. KRISHNA[2], K. HUSSAIN REDDY[1] и G. H. PHILIP[2]

[1]*Department of Chemistry, Sri Krishnadevaraya University Anantapur-515003*
[2]*Department of Zoology, Sri Krishnadevaraya University Anantapur-515003, India*

Синтетисани су мешовито лигандни комплекси никла(II) са 2,4-дихидроксиацетофенон-оксимом (DAPO), 2,4-дихидроксибензофенон-оксимом (DBPO) као примарним лигандима и пиридином (Py), имидазолом (Im) као секундарним лигандима и окарактерисани моларном проводљивошћу, магнетним моментима, електронским, IR и ^{1}H-NMR спектрима. Електрохемијска испитивања извршена су цикличном волтаметријом. Активни сигнали су приписани редокс паровима $Ni^{III/II}$ и $Ni^{II/I}$. Интеракције везивања између металних комплекса и CT DNA изучаване су апсорпцијом и термичком денатурацијом. Активност комплекса према раскидању извршена је на двоструко спиралном pBR322 циркуларном плазмиду DNA коришћењем гел електрофорезе. Сви комплекси показали су повећану нуклеазну активност у присуству оксиданса (H_2O_2). Нуклеазне активности мешовито лигандних комплекса упоређене су са полазним бакар(II) комплексима.

(Примљено 21. јануара, ревидирано 7. октобра 2009)

REFERENCES

1. A. Yan, M. L. Tong, L. N. Ji, Z. W. Mao, *Dalton Trans.* (2006) 2066
2. Y. Z. Cheng, Z. Jing, B. W. Yan, X. Y. Cai, Y. Pin, *J. Inorg. Biochem.* **101** (2007) 10
3. J. K. B. Leigh, M. Z. Jeffrey, *Curr. Opin. Chem. Biol.* **9** (2005) 135
4. D. Shanta, A. N. R. Pattubala, A. R. Chakravarty, *Dalton Trans.* (2004) 697
5. A. Raja, V. Rajendiran, M. P. Uma, R. Balamurugan, C. A. Kilner, M. A. Halcrow, M. Palanaiandavar, *J. Inorg. Biochem.* **99** (2005) 1717
6. L. Lei, N. N. Murthy, T. Joshua, L. Zakharov, P. A. Y. Glenn, L. R. Arnold, D. K. Kenneth, S. E. Rokita, *Inorg. Chem.* **45** (2006) 7144
7. M. A. Halcrow, G. Christou, *Chem. Rev.* **94** (1994**)** 2421
8. P. Stavropoulos, M. C. Muetterties, M. Carrie, R. H. Holm, *J. Am. Chem. Soc.* **113** (1991) 8485
9. G. C. Tucci, R. H. Holm, *J. Am. Chem. Soc.* **117** (1995) 6489
10. I. Tommasi, M. Aresta, P. Giannoccaro, E. Quaranta, C. Fragale, *Inorg. Chim. Acta* **112** (1998) 38
11. U. Ermler, W. Grabarse, S. Shima, M. Goubeaud, R. K. Thauer, *Curr. Opin. Struct. Biol.* **8** (1998) 749
12. F. Dole, M. Medina, C. More, R. Cammack, P. Bertrand, B. Guigliarelli, *Biochemistry* **35** (1996) 16399
13. R. K. Andrews, R. L. Blakeley, B. Zerner, *The Bioinorganic Chemistry of Nickel*, J. R. Lancaster, Ed., VCH Publishers, New York, 1988, p. 141
14. F. Haq, M. C. R. Peter, *J. Inorg. Biochem.* **78** (2000) 217
15. N. Saglam, A. Colak, K. Serbest, S. Dulger, S. Guner, S. Karabocek, A. O. Belduz, *Biometals* **15** (2002) 357
16. M. S. Surendra Babu, K. Hussain Reddy, P. G. Krishna, *Polyhedron* **26** (2007) 572
17. M. E. Reichmann, S. A. Rice, C. A. Thomas, P. Doty, *J. Am. Chem. Soc.* **76** (1954) 3047

18. A. Wolfe, G. H. Shimer, T. Meehan, *Biochemistry* **26** (1987) 6392
19. E. Konig, *The nephelauxetic effect structure and bonding*, Springer, New York, 1971, p. 175
20. C. C. Cheng, S. E. Rokita, C. J. Burrows, *Angew. Chem.* **32** (1993) 273
21. L. A. Lipscomb, F. X. Zhou, S. R. Presnell, R. J. Woo, M. E. Peek, R. R. Plaskon, L. D. Williams, *Biochemistry* **35** (1983) 2818
22. J. Santa Lucia Jr., *Proc. Natl. Acad. Sci. USA* **95** (1998) 1460
23. S. Satyanaryana, J. C. Dabrowiak, J. B. Chaires, *Biochemistry* **32** (1993) 2573
24. R. B. Nair, E. S. Teng, S. L. Kirkland, C. J. Murphy, *Inorg. Chem.* **37** (1998) 139
25. J. Liu, H. Zhang, C. Chen, H. Deng, T. Lu, L. Ji, *Dalton Trans.* (2003) 114
26. Y. M. Song, Q. Wu, P. J. Yang, N. N. Luan, L. F. Wang, Y. M. Liu, *J. Inorg. Biochem.* **100** (2006) 1685.